PROCEEDINGS OF SCIENCE

Limit on an Isotropic Diffuse Gamma-Ray Population with HAWC

John Pretz[*a] **for the HAWC Collaboration**[b]
[a] *Department of Physics, Pennsylvania State University, State College, PA, USA*
[b] *For a complete author list, see www.hawc-observatory.org/collaboration/icrc2015.php*
Email: pretz@psu.edu

Data from 105 days from the High Altitude Water Cherenkov Observatory (HAWC) have been used to place a new limit on an isotropic diffuse gamma-ray population above 10 TeV. High-energy isotropic diffuse gamma-ray emission is produced by unresolved extragalactic objects such as active galactic nuclei, with potential contributions from interactions of high-energy cosmic rays with the inter-Galactic medium, or dark matter annihilation. Isotropic diffuse gamma-ray emission has been observed up to nearly 1 TeV. Above this energy, only upper limits have been reported. Observations or limits of the isotropic photon population above these energies are very sensitive to local astrophysical particle production. Of particular note, we expect a photon population to accompany the TeV-PeV astrophysical neutrino detection seen in the IceCube instrument. Observations or limits of a photon population above this energy can point to the origin of these neutrinos, indicating whether they are within the gamma-ray horizon or not. HAWC, with superior sensitivity to gamma rays between 100 GeV and 100 TeV, continuously observes the overhead sky and will measure or constrain isotropic emission above 1 TeV. We present a limit above 10 TeV based on the background rejection achieved in a 105-day observation of the Crab Nebula with HAWC. The limit will improve substantially with additional data and study.

The 34th International Cosmic Ray Conference,
30 July- 6 August, 2015
The Hague, The Netherlands

[*] Speaker.

1. Motivation

Isotropic diffuse gamma-ray emission can arise from a number of mechanisms including unresolved sources, dark matter[1][2][3], or more exotic phenomena[4][5][6]. Of particular interest are gamma-rays produced in conjunction with the TeV-PeV neutrino population reported by the IceCube collaboration [7][8][9] which may occur in astrophysical pion production or in dark matter annihilation [10]. Charged pion production should be accompanied by neutral pion production and these neutral pions will decay into gamma rays. If the IceCube neutrinos are from pion decay, gamma rays should be produced with a similar spectrum and flux as the neutrinos [11][12]. Gamma rays above 1 TeV that originate outside the galaxy are heavily attenuated by the Extra-Galactic Background Light (EBL). This situation creates a testable hypothesis: A photon flux at the level of the IceCube measurement suggest that the neutrinos are produced locally, within or near our own galaxy [13]. An absence of photons would suggest the neutrinos are produced beyond the gamma-ray horizon [14]. For this reason, diffuse gamma-ray observations are particularly interesting if they reach sensitivity below the level of the IceCube astrophysical neutrino detection.

Electrons and positrons produce similar air showers to gamma rays and appear very similar in a ground array. Cosmic-ray electrons can be accelerated by a nearby pulsar or supernova remnant, but the electrons are isotropized by the intervening magnetic field. Electrons have been observed up to 1 TeV by H.E.S.S. [15]. The spectrum appears to be falling very rapidly, near E^{-4}. The cosmic-ray electron/positron spectrum is interesting in its own right; models suggest that the cosmic-ray electron spectrum may flatten if a nearby source is bright enough [16][17]. It may also constitute a background to photon observation if the spectrum hardens.

The High Altitude Water Cherenkov Observatory (HAWC) is a water-Cherenkov air shower array operating near Sierra Negra in Mexico. A key feature of the high-energy sensitivity of the HAWC instrument is its ability to distinguish electromagnetic air showers from hadronic showers. The 300 4.5-meter deep Water Cherenkov Detectors (WCDs) that make up the instrument are designed for identifying the penetrating particles characteristic of hadronic air showers. HAWC maintains this ability across its entire 20,000 m^2 area.

HAWC is designed to observe localized sources of TeV photons. When observing a localized source, the hadron background is measured from data by interpolating between "off source" observations. When looking for an isotropic population, the hadron background must be determined *a priori* from simulation. HAWC's ability to distinguish hadronic showers from electromagnetic showers is critical. In Section 2 we present some studies of the photon/hadron rejection by looking at the 10 TeV signal from the Crab Nebula. The hadron rejection is so good that we can improve upon existing isotropic photon limits at $\sim$10 TeV without a dedicated isotropic photon analysis. In Section 3, we show the computation of this limit. A number of analysis improvements stand to improve our sensitivity by a factor of 100. Section 4 discusses these prospects.

HAWC cannot easily distinguish between high-energy electrons, positrons and photons. To the extent that air showers from electrons, positrons and photons behave the same, our limits are actually a limit on the combined flux of photons, electrons and positrons. For this analysis, we frame the discussion in terms of gamma rays because we have not yet considered any differences in the air showers generated by electrons or positrons. The prospects for detecting the $\sim$TeV electron/positron population are discussed elsewhere in these proceedings [18].

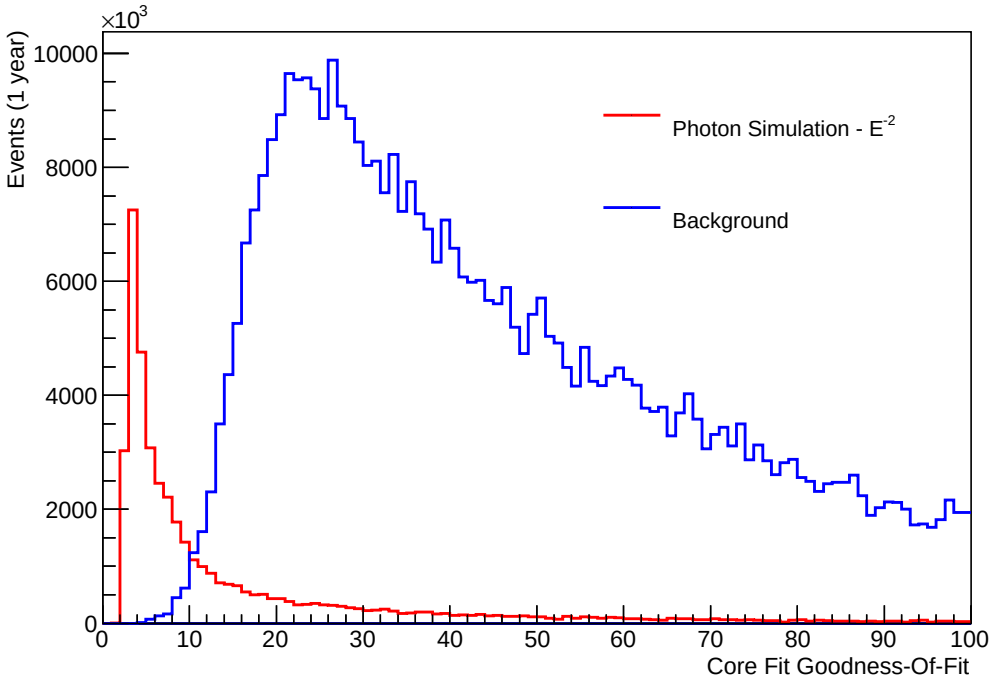

Figure 1: Background separation at 10 TeV with HAWC. The number of events per year is shown as a function of the goodness-of-fit for simulated cosmic rays and gamma rays in HAWC-250. Events with more than 85% of the available PMTs are used. The gamma rays are shown with a simulated spectrum $E^2\Phi(E) = 2000 \cdot 3 \times 10^{-8}$ GeV s^{-1} cm^{-2} sr^{-2}, 2000 times larger than the IceCube neutrino flux.

2. Crab Studies

As the strongest steady TeV source in the sky, the Crab Nebula serves as an important benchmark and calibration source for TeV instruments, including HAWC. The Crab is detected in HAWC data (in the 250-tank configuration) at 38 standard deviations in 150 days of observation [19] and is being used to verify the pointing, stability and energy response of the HAWC instrument. We also use the Crab to evaluate the effectiveness of our photon/hadron discrimination.

Figure 1 exhibits one photon identification variable, a goodness-of-fit measure of the HAWC core reconstruction, described in [20]. It provides excellent separation of photons and hadrons, especially at the high energies we are using for this isotropic photon analysis. The figure corresponds to a photon energy of more than 10 TeV. Photons characteristically have a much lower (i.e. better) goodness-of-fit than cosmic rays, allowing us to distinguish the two.

The efficacy of the hadron rejection is shown most convincingly with real data from the instrument. Figure 2 shows the region around the Crab in 105 days of data with HAWC in its 250-WCD configuration (HAWC-250). For the treatment here, we look at the largest, highest-energy events in HAWC, events which have at least 85% of the available PMTs seeing light. This cut restricts the energy of photon events to roughly $>$10 TeV. Data are shown with a 0.45° top hat smoothing, counting how many events occur within a 0.45°-radius circle around the points shown. The left panel of Figure 2 shows data with more than 85% of the available PMTs seeing light. The right

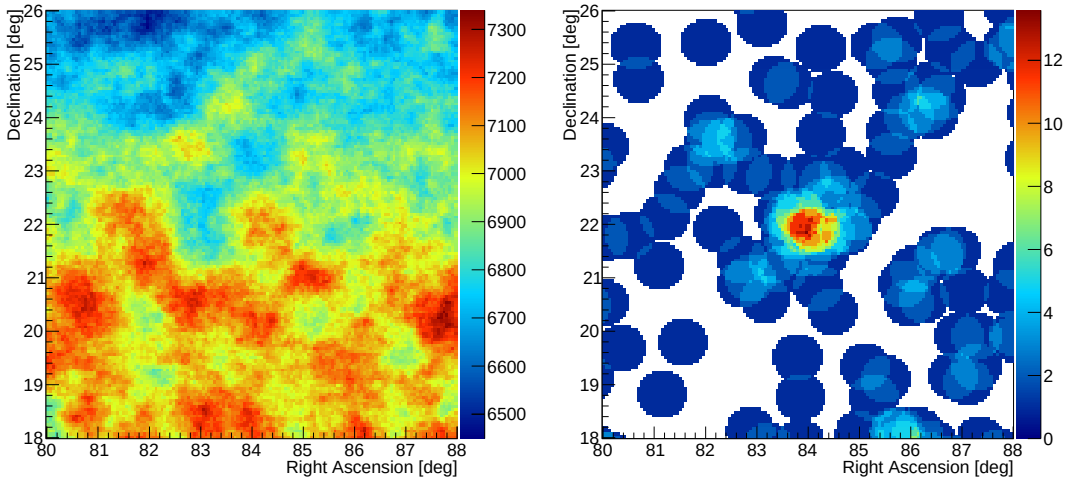

Figure 2: Skymap in equatorial coordinates in the vicinity of the Crab Nebula in 105 days of data with HAWC-250 (shown in the J2014/15 epoch). Events with more than 85% of the available PMTs have been used. The color scale shows the number of events detected within a 0.45° circle around each point in the sky. The left figure shows the region with no cuts and is completely dominated by hadronic cosmic rays. The slight drift in rate is due to the changing acceptance of the detector, located at +19°N latitude, for events further from zenith. The figure on the right shows the same skymap after a strong cut which removes all but 1 in $\sim 10^4$ background events. After cuts, at the location of the Crab, we observe 12 events with an expected background of 0.81 ± 0.05 in this sample.

panel shows the same region of the sky with a strong cut on the core fit goodness-of-fit. The background is suppressed by about 10^{-4} with $\sim$25% efficiency for photons. At these extreme cut levels (very large, very gamma-like events), events are very rare. We record 12 events (in the 0.45° bin) from the direction of the Crab Nebula in 105 days. Using events recorded more than 1° from the Crab, we estimate $0.81 \pm 0.05_{\text{stat}}$ background events.

Figure 3 shows how the Crab excess depends on background rejection. We show measured and predicted event passing rates as a function of the remaining background. The shape agrees well between data and simulation. Because it is time consuming to simulate a full 100 days of experimental data, the background estimate becomes statistically limited at a weaker cut than data. Given the agreement at less-tight levels, we are confident that $\sim$25% gamma-ray efficiency with only 10^{-4} background contamination is achievable, even at this early stage in the analysis. Stronger rejection, and a more pure photon sample, appears possible with harder cuts.

3. Isotropic Gamma-Ray Limit

The strength of the photon/hadron rejection allows us to set a simple, robust limit on an isotropic diffuse gamma-ray flux. Under no circumstances can an isotropic gamma-ray population overproduce the observed off-Crab events. Furthermore, we have a bright gamma-ray source of known flux to normalize our observations.

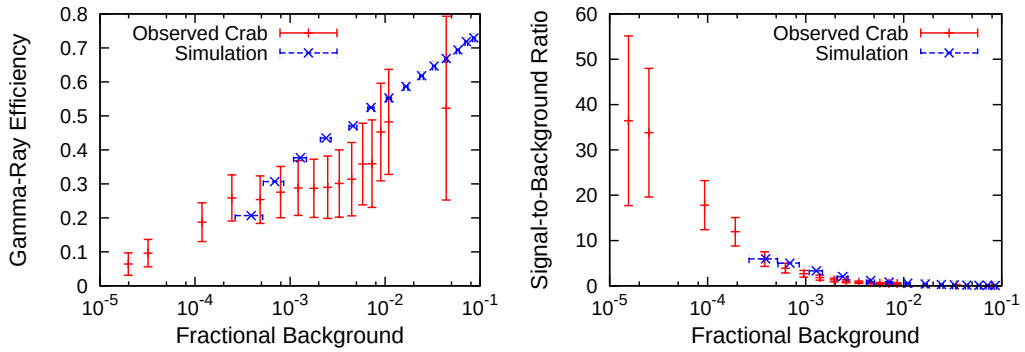

Figure 3: These figures exhibit the performance of the photon/hadron discrimination described in the text. The left panel shows the fraction of the gamma-ray signal expected and measured as a function of the fraction of the background remaining as a cut on the core reconstruction goodness-of-fit is changed. Reasonable cuts produce a background acceptance of 10^{-4} while maintaining an efficiency for gamma-rays of $\sim$25%. The right panel shows the signal-to-background ratio achieved as a function of the fraction of background remaining after cuts.

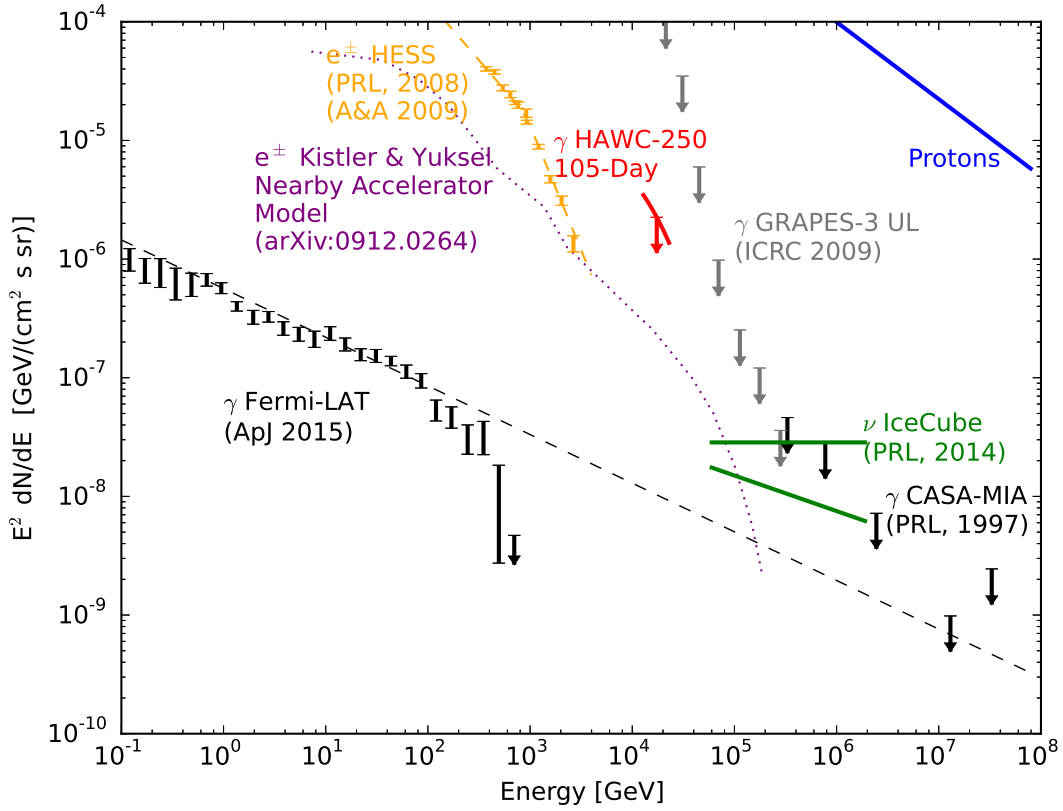

Figure 4: Isotropic diffuse particle limits and measurements of a variety of species [9] [15] [21] [22] [23] and an electron/positron model from [17]. Isotropic gamma-rays have been identified up to $\sim$ 1 TeV by the Fermi-LAT instrument. Above 1 TeV, the most constraining limits come from the GRAPES-3 instrument (in the 10-100 TeV range) and the CASA-MIA experiment (above 100 TeV). The early HAWC limits (shown in red) surpass the GRAPES-3 limits in the 11-23 TeV energy.

Consider F_{Crab}, the point-source differential flux of the Crab at some energy. Assume we measure S events from the Crab in some sample of time. Let us assume the isotropic diffuse emission has the same spectral shape and is given by Φ_{iso} at the same energy as we measure the Crab. Since the isotropic flux is normalized per unit solid angle, a small patch of sky with solid angle Ω_{bin} will produce as many photons as a point source with a flux $\Phi_{\text{iso}}\Omega_{\text{bin}}$. If, in the experiment, we record no more than B events in an Ω_{bin} sized bin, and as long as we are looking near enough to the Crab that the instrument response is flat, then we can say that the isotropic population of photons can be no higher than:

$$\Phi_{\text{iso}} \leq \frac{F_{\text{Crab}}}{\Omega_{\text{bin}}}\frac{B}{S} \tag{3.1}$$

From the Crab observation in Figure 2, we recorded 12 total events at the Crab location, with a background of 0.81 ± 0.05 in a 0.45° round bin. There will be some photons from the Crab outside our 0.45° bin. The bin size was chosen to maximize the statistical significance of the Crab detection and, for a Gaussian-distributed point spread function, that optimum includes only about 70% of the photons. Given the systematic uncertainties introduced by trying to account for these lost events, at this early stage in the analysis, we conservatively perform the limit calculation with the assumption that the total number of Crab events is 11.2.

At 90% confidence, we expect the true mean signal to background ratio on the Crab to be larger than S/B=8.4. Using the H.E.S.S. fit of the differential flux of the Crab [24], we obtain the limit 8.0×10^{-15} cm^{-2} s^{-1} GeV^{-1} sr^{-1} at 17 TeV. Using the HAWC-measured Crab flux yields a similar limit. As we are still evaluating the HAWC systematic errors, we choose to anchor the analysis on a published Crab flux for this study.

The HAWC limit is shown in Figure 4 along with a number of isotropic measurements, limits and models for photons and other particle species. We quote a HAWC limit from $\sim$11-23 TeV, the simulated energy range expected from the Crab for the cuts in this analysis.

4. Discussion and Prospects

The limit presented here is very conservative and essentially comes "for free" from the HAWC observation of the Crab Nebula. It is not representative of what is possible with HAWC, and a number of improvements are possible:

- HAWC data have the potential to constrain higher-energy photons, but we restrict the range of the claimed limit to the energy range over which the Crab is detected in this analysis. As the modeling of the instrument is better understood, this limit will be extended to lower and higher energies. The sensitivity of HAWC at 100 TeV should be at least an order of magnitude better than at 10 TeV.

- We make no attempt to ascribe the observed off-Crab events to hadronic cosmic-rays. This assumption is robust, but very conservative. A stronger limit is possible if some fraction of the remaining background can be demonstrated, through simulation, to be cosmic-ray background. As we understand HAWC better, this will be possible and will improve the sensitivity substantially. Note that we must have some understanding of the background *a*

priori in order to make a positive detection. The analysis presented here can only yield an upper limit.

- We choose a photon/hadron separation cut that results in a convincing Crab detection with an excellent signal to background ratio. As we acquire more data, we will be able to cut harder and further enhance the purity of our sample. Figure 3 suggests that more pure gamma-ray samples are possible. This stands to further improve the results.

The first HAWC limit improves upon the current best limit in the 11-23 TeV range by the GRAPES-3 instrument. Ultimately, we expect to achieve a limit below the level of the IceCube diffuse neutrino flux at 10-100 TeV. HAWC is able to distinguish muons in an air shower across essentially all of its 20,000 m^2 area, more than a factor of 10 larger than CASA-MIA or GRAPES-3.

The limit presented here is formed using the background around the Crab Nebula. Strictly speaking, this limit does not apply to any area of the sky except the immediate vicinity of the Crab. Extending this analysis to the rest of the sky is underway.

Nevertheless, the present limit is the strongest in its energy range. With all the improvements discussed here, future observations will provide a new unique constraint on the combined electron/positron/photon flux. Above 100 TeV, our observations may be able, in the near future, to constrain the origin of the IceCube astrophysical neutrino population.

Acknowledgments

We acknowledge the support from: the US National Science Foundation (NSF); the US Department of Energy Office of High-Energy Physics; the Laboratory Directed Research and Development (LDRD) program of Los Alamos National Laboratory; Consejo Nacional de Ciencia y Tecnología (CONACyT), Mexico (grants 260378, 55155, 105666, 122331, 132197, 167281, 167733); Red de Física de Altas Energías, Mexico; DGAPA-UNAM (grants IG100414-3, IN108713, IN121309, IN115409, IN111315); VIEP-BUAP (grant 161-EXC-2011); the University of Wisconsin Alumni Research Foundation; the Institute of Geophysics, Planetary Physics, and Signatures at Los Alamos National Laboratory; the Luc Binette Foundation UNAM Postdoctoral Fellowship program.

References

[1] L. Bergström, J. Edsjö, and P. Ullio, *Spectral Gamma-Ray Signatures of Cosmological Dark Matter Annihilations*, *Physical Review Letters* **87** (Dec., 2001) 251301, [astro-ph/0105048].

[2] K. N. Abazajian, S. Blanchet, and J. P. Harding, *Current and future constraints on dark matter from prompt and inverse-Compton photon emission in the isotropic diffuse gamma-ray background*, Phys. Rev. D **85** (Feb., 2012) 043509, [arXiv:1011.5090].

[3] P. Ullio, L. Bergström, J. Edsjö, and C. Lacey, *Cosmological dark matter annihilations into γ rays: A closer look*, Phys. Rev. D **66** (Dec., 2002) 123502, [astro-ph/0207125].

[4] P. Bhattacharjee, C. T. Hill, and D. N. Schramm, *Grand unified theories, topological defects, and ultrahigh-energy cosmic rays*, *Physical Review Letters* **69** (July, 1992) 567–570.

[5] A. J. Gill and T. W. B. Kibble, *Cosmic rays from cosmic strings*, Phys. Rev. D **50** (Sept., 1994) 3660–3665, [hep-ph/9403395].

[6] R. J. Protheroe and T. Stanev, *Limits on Models of the Ultrahigh Energy Cosmic Rays Based on Topological Defects*, *Physical Review Letters* **77** (Oct., 1996) 3708–3711, [astro-ph/9605036].

[7] M. G. Aartsen et al., *Evidence for High-Energy Extraterrestrial Neutrinos at the IceCube Detector*, *Science* **342** (Nov., 2013) 1, [arXiv:1311.5238].

[8] M. G. Aartsen et al., *Atmospheric and astrophysical neutrinos above 1 TeV interacting in IceCube*, Phys. Rev. D **91** (Jan., 2015) 022001, [arXiv:1410.1749].

[9] M. G. Aartsen et al., *Observation of High-Energy Astrophysical Neutrinos in Three Years of IceCube Data*, *Physical Review Letters* **113** (Sept., 2014) 101101, [arXiv:1405.5303].

[10] K. Murase, R. Laha, S. Ando, and M. Ahlers, *Testing the Dark Matter Scenario for PeV Neutrinos Observed in IceCube*, *ArXiv e-prints* (Mar., 2015) [arXiv:1503.0466].

[11] T. K. Gaisser, F. Halzen, and T. Stanev, *Particle astrophysics with high energy neutrinos*, Phys. Rep. **258** (July, 1995) 173–236, [hep-ph/9410384].

[12] J. F. Beacom and M. D. Kistler, *Dissecting the Cygnus region with TeV gamma rays and neutrinos*, Phys. Rev. D **75** (Apr., 2007) 083001, [astro-ph/0701751].

[13] M. Ahlers and K. Murase, *Probing the Galactic origin of the IceCube excess with gamma rays*, Phys. Rev. D **90** (July, 2014) 023010, [arXiv:1309.4077].

[14] K. Murase, M. Ahlers, and B. C. Lacki, *Testing the hadronuclear origin of PeV neutrinos observed with IceCube*, Phys. Rev. D **88** (Dec., 2013) 121301, [arXiv:1306.3417].

[15] F. Aharonian et al., *Energy Spectrum of Cosmic-Ray Electrons at TeV Energies*, *Physical Review Letters* **101** (Dec., 2008) 261104, [arXiv:0811.3894].

[16] T. Kobayashi, Y. Komori, K. Yoshida, and J. Nishimura, *The Most Likely Sources of High-Energy Cosmic-Ray Electrons in Supernova Remnants*, ApJ **601** (Jan., 2004) 340–351, [astro-ph/0308470].

[17] M. Kistler and M. Yuksel, *New Constraints on the Highest-Energy Cosmic-Ray Electrons and Positrons*, *ArXiv e-prints* (2009) [arXiv:1410.3696].

[18] S. BenZvi, M. Un Nisa, Z. Hampel, et al., *Measuring the e^+e^- Flux Above 1 TeV with HAWC*, *International Cosmic Ray Conference* (2015).

[19] P. Salesa et al., *Observations of the Crab Nebula with Early HAWC Data*, *International Cosmic Ray Conference* (2015).

[20] A. J. Smith et al., *HAWC Design, Operation, and Analysis*, *International Cosmic Ray Conference* (2015).

[21] M. Ackermann et al., *The Spectrum of Isotropic Diffuse Gamma-Ray Emission between 100 MeV and 820 GeV*, ApJ **799** (Jan., 2015) 86.

[22] M. C. Chantell et al., *Limits on the Isotropic Diffuse Flux of Ultrahigh Energy γ Radiation*, *Physical Review Letters* **79** (Sept., 1997) 1805–1808, [astro-ph/9705246].

[23] M. Minamino et al., *Upper limit on the diffuse gamma ray flux using grapes-3 experiment*, *International Cosmic Ray Conference* (2009).

[24] F. Aharonian et al., *Observations of the Crab nebula with HESS*, A&A **457** (Oct., 2006) 899–915, [astro-ph/0607333].